Check for updates

Space Weather

RESEARCH ARTICLE
10.1029/2026SW004966

Geomagnetically Induced Currents, Transformer Harmonics, and Reactive Power Impacts: Observed Response of a Single-Phase Transformer in New Zealand

Xinhu Feng[1], C. J. Rodger[1], M. A. Clilverd[2], D. H. Mac Manus[1], Victor Lo[3], M. Dalzell[3], A. Renton[3], A. Lapthorn[4], J. B. Brundell[1], and Tanja Petersen[5]

[1]Department of Physics, University of Otago, Dunedin, New Zealand, [2]British Antarctic Survey (UKRI- NERC), Cambridge, UK, [3]Transpower New Zealand Limited, Wellington, New Zealand, [4]Department of Electrical and Computer Engineering, University of Canterbury, Christchurch, New Zealand, [5]Department of Science Operations & Data, Earth Sciences New Zealand, Lower Hutt, New Zealand

Abstract Geomagnetic storms represent a space weather hazard to power transmission networks due to the effects of induced geo-electric fields within the conducting surface of the Earth. These drive electric currents in power transmission lines which can flow to ground through the neutral-ground connections of transformers. Geomagnetically induced currents (GIC) can negatively impact the operation of high voltage transformers through asymmetric half-cycle transformer core saturation. In this study GIC measurements, derived effective current, and reactive power responses (Q) of the single-phase bank autotransformer, T4, operating at 220 kV in the Halfway Bush substation, Dunedin, New Zealand have been analyzed over the period 2013–2017. During 8 elevated GIC events linear enhancements of reactive power consumption (Q_{con}, MVAr) occurred, even with comparatively low levels of GIC (i.e., <7 A). This is consistent with transformer core saturation where there is little tolerance or "headroom" to GIC in the design for single-phase bank transformers. Reactive power measurements show high variability. The removal of the non-GIC variability is difficult and introduces uncertainty into the identification of GIC-driven responses. In this analysis we consider two techniques to isolate GIC-induced reactive power responses. We find that transformer T4 exhibited a reactive power response of ∼0.115 MVAr/A. The results are a factor of 2–3 larger than MVAr changes in a nearby three-phase, three-limb autotransformer, aligning with previous research. The results are consistent with, but less extreme than modeling studies found for transformer units operating at significantly higher voltages.

Plain Language Summary During large geomagnetic storms high levels of quasi DC currents can be induced in long, low resistance, high voltage power lines. In this study reactive power consumption was observed to increase with increasing DC levels in a single-phase transformer. Over a period of 5 years 8 geomagnetic storm events generated induced currents (GIC) at levels high enough to cause partial saturation of the transformer core under study and, as a result, increased reactive power consumption was detected. Such measurements of the response of transformers to induced DC are rare in scientific and engineering literature. The results presented here provide key understanding of the response of a commonly used transformer-type to geomagnetically induced currents driven by space weather events.

Key Points:

- Geomagnetically induced current (GIC) measurements were analyzed for a single-phase autotransformer, operating at 220 kV in New Zealand
- In Halfway Bush substation, Dunedin, GIC-induced reactive power consumption (Q_{con}) was identified in 8 geomagnetic storms over 5 years
- GIC-induced Q_{con} occurred for GIC ≥ 7 A, with larger increases in MVAr for increasing GIC when compared with 3-phase, 3-limb transformers

Supporting Information:

Supporting Information may be found in the online version of this article.

Correspondence to:

M. A. Clilverd,
macl@bas.ac.uk

Citation:

Feng, X., Rodger, C. J., Clilverd, M. A., Mac Manus, D. H., Lo, V., Dalzell, M., et al. (2026). Geomagnetically induced currents, transformer harmonics, and reactive power impacts: Observed response of a single-phase transformer in New Zealand. *Space Weather*, *24*, e2026SW004966. https://doi.org/10.1029/2026SW004966

Received 27 JAN 2026
Accepted 21 MAY 2026

Author Contributions:

Conceptualization: C. J. Rodger
Data curation: D. H. Mac Manus, Victor Lo, M. Dalzell, J. B. Brundell, Tanja Petersen
Formal analysis: Xinhu Feng, M. A. Clilverd, D. H. Mac Manus, Victor Lo
Funding acquisition: C. J. Rodger
Methodology: C. J. Rodger, M. A. Clilverd, A. Lapthorn, J. B. Brundell
Project administration: C. J. Rodger, A. Renton
Resources: M. Dalzell, A. Renton, J. B. Brundell, Tanja Petersen

© 2026. The Author(s).
This is an open access article under the terms of the Creative Commons Attribution License, which permits use, distribution and reproduction in any medium, provided the original work is properly cited.

1. Introduction

During large geomagnetic storms geo-electric fields induced within the conducting surface of the Earth can drive electric currents in power transmission lines (Beggan et al., 2013; Birkeland, 1908; Divett et al., 2017; Rodger et al., 2017; Vasseur & Weidelt, 1977). Such geomagnetically induced currents (GIC) can flow through a power transmission network to ground via neutral-ground connections in transformers (Divett et al., 2020; Mac Manus et al., 2022). GIC variations occur at a much lower frequency than the power system frequency so appear as quasi-dc currents to the transformers. Quasi DC GIC acts through asymmetric half-cycle transformer core saturation (Arrillaga & Watson, 2003; Rodger et al., 2020). The effect of GIC on impacted transformers is seen through increased reactive power consumption (Q_{con}), and AC waveform distortion (Boteler et al., 1989; Clilverd et al., 2025; Crack et al., 2024; Rodger et al., 2020), resulting in potential voltage collapse, or transformer damage due to internal heating (Boteler, 2015; Samuelsson, 2013).

Supervision: C. J. Rodger
Validation: D. H. Mac Manus
Visualization: Xinhu Feng, M. A. Clilverd
Writing – original draft: M. A. Clilverd
Writing – review & editing: C. J. Rodger, D. H. Mac Manus, Victor Lo, M. Dalzell, A. Renton, A. Lapthorn, J. B. Brundell

Power transformers in New Zealand come in two common configurations. Three-phase, three-limb transformers and single-phase transformers. The response of transformers to GIC is a key factor in the impact of geomagnetic storms on power transmission networks. Reactive power responses to varying levels of GIC, including thresholds at which increased reactive current draw occurs, is a function of the saturation curve of the transformer. Through design, some transformers have a level of headroom before they start to enter saturation. However, there are few measurements defining the response of susceptible transformers, and the majority of current insight is gained from modeling efforts (e.g., Bonmann et al., 2024; Dong et al., 2001; Price, 2002; Rezaei-Zare et al., 2016). Typically, modeling studies give estimates of 0.08–0.29 MVAr/A once the neutral current threshold, that is, headroom, is exceeded. Clilverd et al. (2025) studied the GIC responses of a pair of three-phase, three-limb transformers during the May 2024 Gannon storm. GIC levels of up to 113 A were measured, with multiple short-lived (minutes-long) events occurring over a 14 hr period. A saturation headroom threshold of ∼30 A per transformer was observed, with linear reactive power consumption responses of 0.03–0.04 MVAr/A thereafter. Large differences between modeled and measured reactive power consumption responses to GIC makes estimation of network susceptibility to geomagnetic storm activity uncertain, which is important to determine the hazard posed by space weather to power grid hardware.

Single-phase transformers are expected to be more susceptible to GIC than three-phase, three-limb transformers (e.g., Dong et al., 2001). Using a simplified model based on an equivalent magnetizing current curve Dong et al. (2001) undertook modeling which found a Q_{con}-GIC slope of 1.18 MVAr/A for single-phase transformers which compared with only 0.29 MVAr/A from their modeling for three-phase, three-limb transformers, that is, a factor of ∼4 in relative responsiveness. Marti et al. (2013) and Rezaei-Zare (2014) developed separate analytical modeling approaches to describe the GIC responses of transformers, both of which showed the importance of the operational voltage. Larger reactive power responses to GIC were calculated for higher operational voltages, particularly for single-phase transformers. Marti et al. (Figure 5, 2013) showed that for an operational voltage of 500 kV a single-phase transformer would be expected to have a reactive power consumption response of ∼0.4 MVAr/A when experiencing elevated GIC.

The single-phase transformer at Halfway Bush substation (HWB) in Dunedin, New Zealand failed and required repair as a result of a 2001 geomagnetic storm (Marshall et al., 2012) that produced an estimated 100 A GIC flowing to ground through the transformer (Rodger et al., 2017). Following the decommissioning of HWB T4 in late 2017, subsequent moderate geomagnetic storms have been observed to produce lower levels of observed AC waveform distortion than in previous geomagnetic disturbances, suggesting less asymmetric saturation happening in the remaining three-phase, three-limb transformer units (Clilverd et al., 2020; Crack et al., 2024). This was consistent with the suggestion of single-phase transformers being more susceptible than the three-phase, three-limb type, thereby generating most of the observed harmonic distortion.

In this study we analyze reactive power measurements made at the single-phase autotransformer, T4, in the Halfway Bush substation (HWB) in Dunedin, New Zealand. During the period 2013–2017 a total of 8 short periods of enhanced GIC were observed, leading to reactive power increases. The relationship between GIC level and reactive power consumption is determined for each GIC event after deriving the effective current impacting the autotransformer. This analysis provides insight into the reactive power response of a single-phase transformer during geomagnetic storms. Section 2 describes the GIC and reactive power data sets from Halfway Bush substation. Section 3 investigates the reactive power responses to the GIC events as well as the two baseline techniques used to remove the normal reactive power variations and determine the reactive power consumption changes. The results section, 4, is sub-divided into a further three parts. Sections 4.1 and 4.2 undertake case-study reactive power analysis for two GIC events when measurements from both T4 and T6 are available. Section 4.3 describes the reactive power analysis when only T4 measurements were available. Discussion and Conclusions are presented in Sections 5 and 6.

2. Halfway Bush Substation Data Sets

The response of the single-phase T4 autotransformer in the HWB substation, Dunedin, New Zealand, to geomagnetic storms and their consequently enhanced GIC levels has been captured by a series of measurements made within the substation over a number of years. T4 had a star (wye) winding configuration with a neutral-ground connection, and an operational voltage of 220 kV. Transpower New Zealand Ltd, equipped T4 with a LEM neutral-earth current monitor (Mac Manus et al., 2017; Rodger et al., 2020), and measured T4 reactive

15427390, 2026, 6, Downloaded from https://agupubs.onlinelibrary.wiley.com/doi/10.1029/2026SW004966 by British Antarctic Survey, Wiley Online Library on [17/06/2026]. See the Terms and Conditions (https://onlinelibrary.wiley.com/terms-and-conditions) on Wiley Online Library for rules of use; OA articles are governed by the applicable Creative Commons License

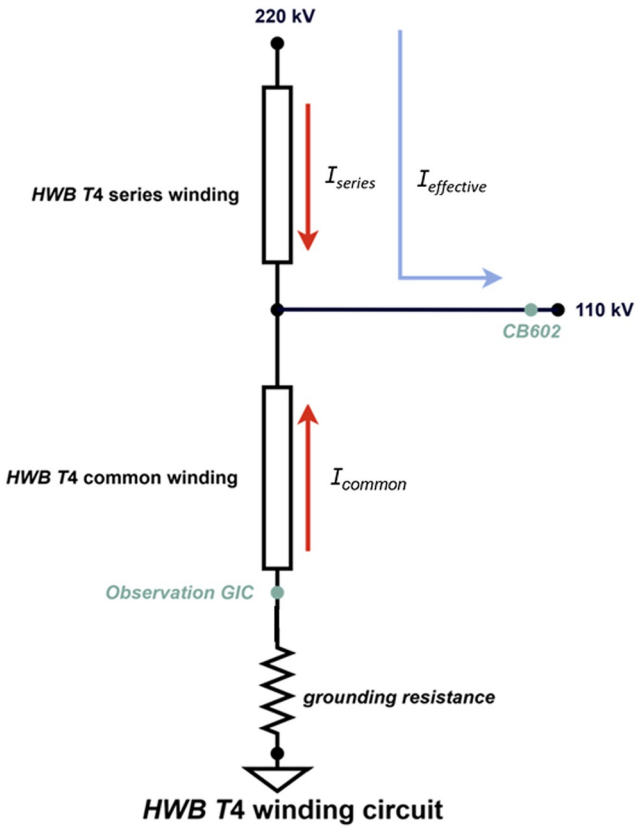

Figure 1. A winding circuit schematic of the T4 autotransformer showing the common and series windings. Also shown are the location of the GIC observations, and the location of the circuit breaker (CB602) where reactive power measurements were made. Reactive power at T4 is derived from metering at circuit breaker CB602 on the 110 kV bus, this measurement includes the combined reactive power of T4 and the connected 110 kV network, from which the GIC-driven component Q_{con} is isolated using the T6 scaling method described in Section 3. $I_{effective}$ is an equivalent current that would give the same magnetomotive force as the combined series and common winding currents. It is not independently measurable, but is shown here for conceptual clarity and is differentiated from the other currents by being depicted in blue rather than red.

power at circuit breaker CB602 as identified in the line diagram of HWB shown in the upper panel of Figure 8 of Clilverd et al. (2018). GIC measurements at T4 were undertaken from October 2012 up to its decommissioning in late 2017. The 8 events analyzed in this study were selected on the basis that the peak effective GIC in T4 exceeded 15 A, rather than on a specific geomagnetic storm classification criterion such as a Dst index threshold. This reflects the fact that GIC amplitude at a specific network location depends not only on storm intensity but also on the orientation and spatial scale of the driving geo-electric field relative to the transmission network topology.

From June 2015 until the decommissioning of T4 in November 2017, a three-phase, three-limb autotransformer, T6, operated alongside T4 in HWB (Clilverd et al., 2020; Crack et al., 2024). Monitoring of T6 with GIC data also provided by a LEM neutral current monitor, and reactive power measured by circuit breaker CB592, shown in the HWB line diagram in Figure 2 of Clilverd et al. (2025). Three of the eight GIC events mentioned above occurred when both T4 and T6 were operating. The three-phase, three-limb autotransformer, T6, has been shown to respond to GIC when it experiences a neutral-earth current ≥30 A (Clilverd et al., 2025). In that study the response was evidenced by enhanced harmonic amplitudes and increased reactive power consumption. By comparing the reactive power changes in T6 and T4 when T6 GIC <30 A it is possible to identify the GIC-induced reactive power response of the single-phase autotransformer T4 alone.

HWB T4, is a bank of single phase autotransformers. Autotransformers have only one winding for each phase bank and therefore the primary and secondary windings share a portion of the turns. These are known as series and common windings (Boteler & Pirjola, 2017). Due to their common and series winding structure the measured GIC at the transformer neutral—ground connection does not fully represent the true level of the quasi-DC current that can impact the transformer.

It is necessary to distinguish between three current quantities used in this study. A schematic of the T4 winding circuit is shown in Figure 1. The common winding GIC (I_{common}) is the quasi-DC current measured directly at the transformer neutral–ground connection. The measurement is made by a LEM neutral-earth current monitor and represents the GIC entering the transformer through the grounded neutral. The series winding GIC flowing through the high-voltage winding section (I_{series}) is not measured; I_{series} is estimated from I_{common} via winding ratio (μ_K). The effective GIC (I_{eff}) combines both winding currents weighted by their respective turn counts leading to an equivalent current parameter representing the total magnetomotive force driving core saturation. All GIC levels presented in this study are expressed as I_{eff} unless otherwise stated.

Albertson et al. (1981) introduced an effective GIC parameter to take account the different GIC values in the series and common windings of an autotransformer. The IEEE Std C57.163™-2023 confirms that effective GIC is the foundation for defining transformer performance characteristics during space weather events, thereby quantifying the risk caused by GIC. Calculation of effective GIC for different types of transformers have been presented by several authors. These different formulas are collected into a common structure in: Boteler and Pirjola (2017). We use the Patil (2014) formula for calculating the effective GIC in two-winding autotransformers. It should be noted that HWB T4 is a three winding autotransformer. However, the third, 11 kV, winding of T4 is delta-connected and does not provide a path for the flow of DC or quasi-DC currents such as GIC. Therefore, the calculation of effective current using the formulation for a two-winding transformer is appropriate.

The two winding autotransformer method for calculating effective GIC computes a proportionality factor, $\mu_{K_{model(t)}}$ by taking the ratio of the modeled series winding and common winding GICs:

15427390, 2026, 6, Downloaded from https://agupubs.onlinelibrary.wiley.com/doi/10.1029/2026SW004966 by British Antarctic Survey, Wiley Online Library on [17/06/2026]. See the Terms and Conditions (https://onlinelibrary.wiley.com/terms-and-conditions) on Wiley Online Library for rules of use; OA articles are governed by the applicable Creative Commons License

10.1029/2026SW004966

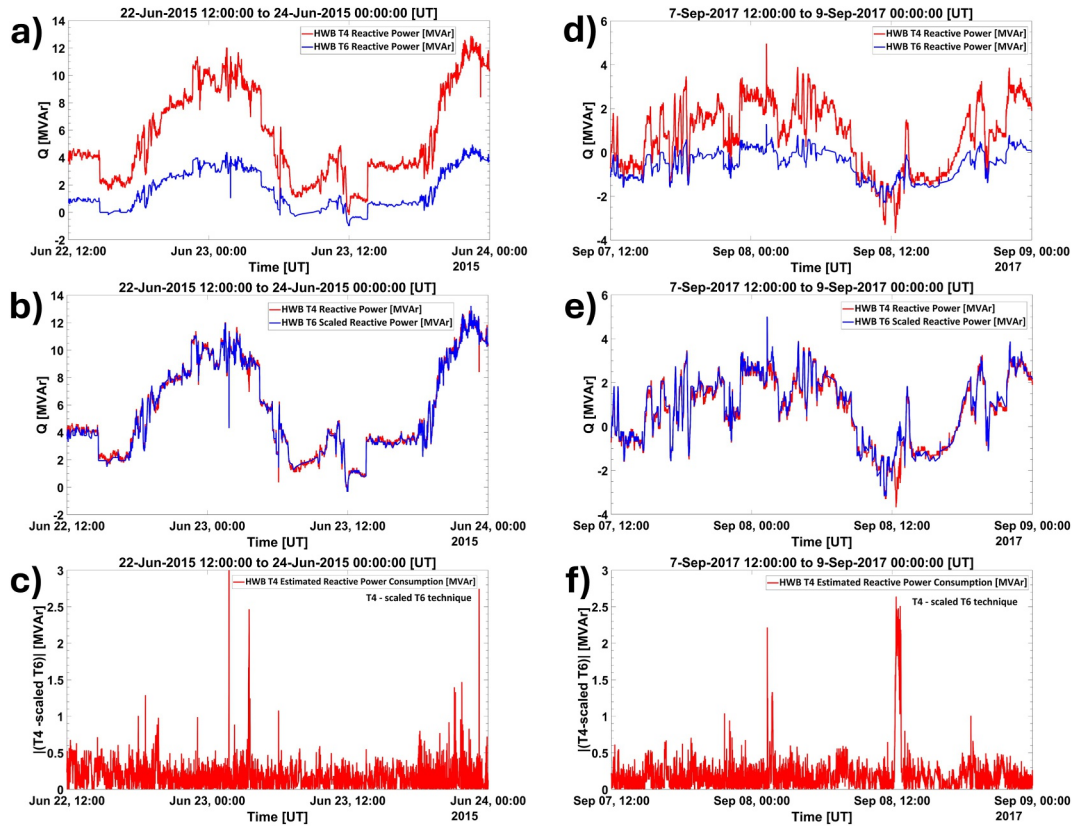

Figure 2. The variation of reactive power, Q, for T4 and T6 in Halfway Bush substation, Dunedin, NZ. Panels (a) and (d) show 2 days of measurements from 22—24 June 2015, and 07–09 September 2017 respectively. T4 data in red, and T6 data in blue. Panels (b) and (e) show the result of scaling the T6 Q values to provide a best overall fit to the T4 Q values for each time period. Panels (c) and (f) show the difference between the T4 Q values, and the scaled T6 values. Typical noise levels of ∼0.5 MVAr are seen with occasional peaks of ∼2–3 MVAr.

$$\mu_{K_{\text{model}(t)}} = \frac{I_{\text{series-model}}(t)}{I_{\text{common-model}}(t)} \tag{1}$$

where,

$I_{\text{series}-\text{model}}(t)$: modeled GIC on series winding.

$I_{\text{common}-\text{model}}(t)$: modeled GIC on common winding.

The flow of GIC is a quasi-DC phenomenon governed entirely by power network DC resistance and topology. Therefore, the ratio of currents between the windings is a fixed characteristic of the autotransformer and its connection to the grid. The highly validated transformer-level GIC model of the New Zealand power network (explained extensively in Divett et al., 2017, 2018, 2020) was used to calculate the proportionality factor for each of the 8 events studied here, covering a period of 5 years. The transformer-level GIC model represents the New Zealand South Island 220 kV transmission network as a resistive DC circuit, with nodes at substations and branches representing transmission lines and transformer windings. Input parameters provided by Transpower New Zealand include the DC resistance of each transmission line segment, the winding DC resistances of each transformer, and substation grounding resistances. Geo-electric fields derived from geomagnetic observatory data at Eyrewell (EYR) are applied as driving voltages along each transmission line segment using the standard line-integral formulation. The model has been extensively validated against direct GIC measurements at multiple New Zealand substations (Divett et al., 2017, 2020; Mac Manus et al., 2022). In the present study, the model is used solely to determine the winding current ratio for the T4 and T6 autotransformers, which is required to convert measured neutral-ground GIC into effective GIC.

15427390, 2026, 6, Downloaded from https://agupubs.onlinelibrary.wiley.com/doi/10.1029/2026SW004966 by British Antarctic Survey, Wiley Online Library on [17/06/2026]. See the Terms and Conditions (https://onlinelibrary.wiley.com/terms-and-conditions) on Wiley Online Library for rules of use; OA articles are governed by the applicable Creative Commons License

15427390, 2026, 6, Downloaded from https://agupubs.onlinelibrary.wiley.com/doi/10.1029/2026SW004966 by British Antarctic Survey, Wiley Online Library on [17/06/2026]. See the Terms and Conditions (https://onlinelibrary.wiley.com/terms-and-conditions) on Wiley Online Library for rules of use; OA articles are governed by the applicable Creative Commons License

Highly consistent proportionality values were found, such that $\mu_{K_{\text{model}(t)}} = 0.41 \pm 0.01$ with only a few of the >1,200 individual values lying outside of the 0.41 ± 0.01 range. This is a somewhat unexpected result in that the network resistances seen at the T4 terminals will in principle vary as a result of the spatial structure of the magnetic disturbance. However, the proportionality factor results presented here for T4 involve case studies that assume a spatially uniform magnetic field across the network, determined using Eyrewell magnetometer data only (as it was the only measurement available at the time). Hence the small range of values stated.

The GIC measurements for the HWB T4 autotransformer are taken on the common winding and can be converted to the series winding current using the proportionality factor:

$$I_{\text{series-Estimated}}(t) = \mu_{K_{\text{model}(t)}} \times I_{\text{common-measured}}(t) \tag{2}$$

where,

$I_{\text{series-Estimated}}(t)$: the series winding GIC.

$I_{\text{common-measured}}(t)$: observed GIC measurements on the common winding.

Using the two-winding autotransformer formulation presented in Patil (2014) the effective GIC, I_{eff}, can be written as:

$$I_{\text{eff}} = \left| \frac{(N-1)\, I_{\text{series}} + I_{\text{Common}}}{N} \right|, N = \frac{V_1}{V_2} \tag{3}$$

The operational voltages for T4 are $V_1 = 220$ kV, $V_2 = 110$ kV, therefore $N = \frac{V_1}{V_2} = 2$.

The expression can be further derived to:

$$I_{\text{eff}} = \left| \frac{I_{\text{series}} + I_{\text{common}}}{2} \right| = \frac{\mu_{K_{\text{model}(t)}} * I_{\text{common-measured}}(t) + I_{\text{common-measured}}(t)}{2}$$

Thus, for T4 we find that $I_{\text{eff}} = I_{\text{common}} \left| \frac{0.41+1}{2} \right| = 0.705\, I_{\text{common}}$

Throughout this study we convert the measured GIC levels provided for T4 by Transpower (Manus Mac et al., 2017; Rodger et al., 2017, 2020) by applying a conversion factor of 0.705. The T6 three-phase, three-limb transformer is also an autotransformer. Using the same technique as outlined for T4 above, we find that the modeled series windings during the three coincident study events is 0.84 ± 0.01 for T6. Thus, we can write $I_{\text{eff}} = 0.92\, I_{\text{common}}$ for T6. The figures shown in this study are plotted with I_{eff} throughout.

In Appendix A a specific autotransformer conversion factor for T6 is calculated during the May 2024 Gannon geomagnetic storm period. This revised factor takes into account the different network topology in 2024 compared to the 2013–2017 study period, that is, T4 had been removed before 2024, and T3 was installed after 2017. The importance of the T6 conversion is in adjusting the transformer saturation headroom of 30 A found using the measured GIC during that particular storm in 2024 (Clilverd et al., 2025) into a T6 headroom value for I_{eff} which is a more relevant measure for the longer-term analysis undertaken here. For the T6 three-phase, three-limb autotransformer the headroom threshold in 2024 is found to be $I_{\text{eff}} = 24$ A rather than the 30 A measured for the common winding-only. The assumption being that the I_{eff} headroom value remains constant over time. This result directly relates to the assumption that by comparing the reactive power changes in T6 and T4 when T6 $I_{\text{eff}} < 24$ A during 2013–2017 it is possible to identify the GIC-induced reactive power response of T4 alone.

In this study we use the four data sets mentioned above, that is, T4 GIC and reactive power as well as T6 GIC and reactive power. The time samples of the raw data sets are typically separated by 4–30 s. Samples occur with different timing gaps occurring in each of the data sets. In order to provide comparative measurements the data sets were interpolated with a uniform 5 s time resolution. The analysis undertaken is performed with the interpolated data sets.

15427390, 2026, 6, Downloaded from https://agupubs.onlinelibrary.wiley.com/doi/10.1029/2026SW004966 by British Antarctic Survey, Wiley Online Library on [17/06/2026]. See the Terms and Conditions (https://onlinelibrary.wiley.com/terms-and-conditions) on Wiley Online Library for rules of use; OA articles are governed by the applicable Creative Commons License

3. Reactive Power Measurements

Measured reactive power levels associated with the HWB T4 and T6 transformer operation show high variability. This is shown in Figures 2a and 2d, where multiple days of reactive power measurements (Q) from T4 (red line) and T6 (blue line) are plotted. The periods presented cover 22–24 June 2015, and 05–09 September 2017. The majority of the variations shown are normal reactive power background variations that arise from the normal power-system operation. The normal background can vary due to a range of operational factors such as network loading, and reactive compensation. Therefore, a background-removal step is required to better isolate the GIC-related reactive power enhancements. A diurnal variation in reactive power is seen in Figures 2a and 2d. The peak each day occurs at ∼00 UT, which, because of the difference between UT and LT, is consistent with high local noon demand (00 UT), and a minimum around local midnight (12 UT).

The 22–24 June 2015 period is associated with a large geomagnetic storm reaching a minimum Dst of ∼−200 nT. The 07–09 September 2017 geomagnetic storm reached a minimum Dst of ∼−150 nT and has been the subject of previous HWB-focused analysis (Clilverd et al., 2018, 2020). In both panels the T4 reactive power varies over ∼12 MVAr, while for T6 there is a much smaller variation. It is clear, however, that the reactive power from both transformers varies in a nearly identical way during the majority of the multi-day time periods, just with different amplitudes.

Figures 2b and 2e shows the result of scaling the T6 normal reactive power values to the same range as the T4 values, where scaling values were applied that maximizes the overlap of the two data sets. The T6 reactive power was scaled to match the dynamic range of T4 using a quantile-based linear mapping. The 1st and 99th percentiles of Q_{T4} and Q_{T6} were computed over the full multi-day analysis window, and a linear transformation Q_{con} (t) = Q_{T4} (t)-$Q_{(T6\text{-}scaled)}$ (t) was determined by mapping the T6 percentile range onto the T4 percentile range. This approach is robust to short-lived GIC-driven outliers, which constitute only a small fraction of the normal variations of reactive power and have negligible influence on the percentile values. The stability of the scaling was confirmed by repeating the procedure with five alternative quantile pairs (2%/98% through 20%/80%): the quiet-time residual standard deviation remained below 0.24 MVAr in all cases. The Pearson correlation between Q_{T4} and $Q_{T6\text{-}scaled}$ during quiet periods was ≥0.9966 for every quantile pair.

The results of subtracting the scaled T6 reactive power values from the T4 values are shown in Figures 2c and 2f. The absolute difference between T4 and scaled T6 reactive power typically exhibits variations of <0.5 MVAr. However, differences of ∼2–3 MVAr occur occasionally. These periods can be thought of as times when the transformers T4 and T6 respond differently to operational conditions. Such periods would be expected during geomagnetic storms when GIC levels are elevated, because single-phase (i.e., T4) and three-phase, three-limb (i.e., T6) transformers are likely to respond differently, with T4 being more responsive to GIC than T6 (Clilverd et al., 2020). Clilverd et al. (2025) showed that the three-phase, three-limb transformer at HWB, T6, only starts to show reactive power consumption (Q_{con}) responses when the measured neutral-ground GIC (for the common winding) exceeds 30 A. As discussed in Section 2 and Appendix A, because T6 is an three-phase, three-limb autotransformer, Q_{con} for T6 would only be expected to respond when $I_{eff} \geq 24$ A. Thus the 2–3 MVAr differences between T4 reactive power and the scaled T6 values could be associated with periods when elevated GIC are present but $I_{eff} < 24$ A in T6, that is, reactive power consumption in T4 would respond to the GIC but T6 would not. In the next sections we use this characteristic to identify the single-phase, T4, reactive power consumption response to effective GIC.

4. Results

In the following results section, Sections 4.1 and 4.2 analyze in detail two case-study periods where T6 measurements are available. The relationships determined between reactive power and GIC are shown in Figures 5 and 8 respectively. In Sections 4.1 and 4.2 we use the T4—scaled T6 technique to estimate the T4 reactive power response to effective GIC, using the scaled T6 reactive power to identify the normal background reactive power levels for T4 during the GIC events. These results are compared with a more simple linear estimate technique to work out the background levels. In Section 4.3 a stand-alone linear estimate of the background T4 reactive power during 5 short-lived GIC events is made in the absence of T6 reactive power data. The relationships between reactive power and GIC for those events are shown in Figure 10.

15427390, 2026, 6, Downloaded from https://agupubs.onlinelibrary.wiley.com/doi/10.1029/2026SW004966 by British Antarctic Survey, Wiley Online Library on [17/06/2026]. See the Terms and Conditions (https://onlinelibrary.wiley.com/terms-and-conditions) on Wiley Online Library for rules of use; OA articles are governed by the applicable Creative Commons License

4.1. June 2015 Case-Study Event With T6 Present

On 23 June 2015 enhanced neutral-ground GIC occurred in both T4 and T6 transformers at HWB. The single-phase autotransformer T4 experienced effective GIC as high as 30 A, whereas for the three-phase, three-limb autotransformer, T6, effective GIC peaked at 28 A. The time variation of absolute effective GIC over a 2 hr period is shown in Figure 3a. For both T4 and T6 the variations of effective GIC during the event are very similar. Reactive power variations for T4 (red line) and scaled T6 (black line) are shown over the same 2-hr period in Figure 3b. When effective GIC levels are close to 0 A the two traces vary in much the same way. However, during the enhanced GIC period, there is a noticeable difference between the reactive power exhibited by T4 and those of the scaled T6. As discussed in Section 2 and Appendix A, T6 only shows GIC induced reactive power responses when the effective GIC $\geq$ 24 A. Thus, as the T6 effective GIC levels are <24 A for the majority of this event, the scaled T6 reactive power can be thought of as representing the non-enhanced background reactive power consumption level for T4. Alternatively, Figure 3c shows the T4 reactive power variation (blue line) with an estimate of the non-disturbed background reactive power level made by a straight line connecting times of zero effective GIC either side of the event as identified by vertical dashed lines in all of the panels—we term this the linear estimated background reactive power.

The result of removing the non-disturbed background from the T4 reactive power levels during the 23 June 2015 GIC event are shown in Figures 4a and 4b. Figure 4a shows the reactive power consumption (Q_{con}) determined from the scaled T6 technique (red line), with peak values of ~2.5 MVAr. Elevated Q_{con} lasts for ~10 min Figure 4b shows Q_{con} determined using the linear estimated technique (blue line). Similar temporal variations can be seen in the two panels, although the Q_{con} only reaches ~2 MVAr using the linear estimate assumption.

Once Q_{con} has been isolated using the two different background estimation techniques it is possible to determine their reactive power consumption relationships with effective GIC level. Figure 5a shows the result for the scaled T6 technique (red dots), while Figure 5b shows the result for the linear estimate technique (blue dots). In both cases values are only plotted from within the event period, as indicated by the green dashed lines shown in Figure 4. In this figure, and in further figures showing the reactive power consumption relationship with effective GIC, a 10 s delay is applied between each GIC measurement and the reactive power measurement. The 10 s delay was adopted directly from Bolduc et al. (2000), who identified a 10-s lag between GIC and the resulting reactive power response in their study of a transformer in the Hydro-Québec system. We applied this value to our analysis on the basis that a similar physical delay, arising from the finite time required for the transformer core to reach a new saturation state following a change in GIC, might be expected for T4. This adopted value was independently verified by our own cross-correlation analysis of the GIC and Q_{con} time series for the events analyzed in this study.

For T4 effective GIC levels <7 A no clear increase in Q_{con} is observed with either background estimation technique. For T4 effective GIC levels from 7 to 30 A the scaled T6 technique exhibits an increasing Q_{con} with increasing GIC level. The slope of the line of best fit for GIC $\geq$ 7 A is 0.118 MVAr/A with a Pearson correlation coefficient of ~0.92 (solid black line). Using the linear estimate assumption a similar relationship can be seen, and a best fit slope of 0.085 MVAr/A is found, with a Pearson correlation of ~0.80. The lack of a trend in Q_{con} for GIC < 7 A can be thought of as the T4 transformer designed "headroom" for DC currents flowing within the transformer windings. For the rest of the analysis presented in this study, the T4 7 A headroom value is identified by a vertical dashed line in the relevant plots, with best fit lines with correlations only calculated for GIC $\geq$7 A.

4.2. September 2017 Case-Study Event With T6 Present

Shortly after 12 UT on 08 September 2017 large GIC were measured at HWB T4 and T6. Figure 6a shows the absolute variation of effective GIC in both transformers (T4 in black, T6 in blue) during a 2-hr window, 11:30–13:30 UT, 08 September 2017. For both T4 and T6 the variations of effective GIC during the event are very similar. The study period (labeled: Event 4 period B) is identified by the horizontal green line. This restricted period was selected for analysis because the majority of theT6 effective GIC were typically <24 A (see Section 2 and Appendix A) and thus no significant reactive power changes caused by T6 would be expected (Clilverd et al., 2025). Any reactive power changes detected above a non-disturbed baseline would therefore be expected to be as a result of a T4 response to the GIC. The large spike in GIC after ~12:45 UT has T6 effective GIC $\geq$24 A as well as T4 $\geq$7 A, and so would likely cause a reactive power response in both transformers. As such, this latter period of high GIC is excluded from the present analysis.

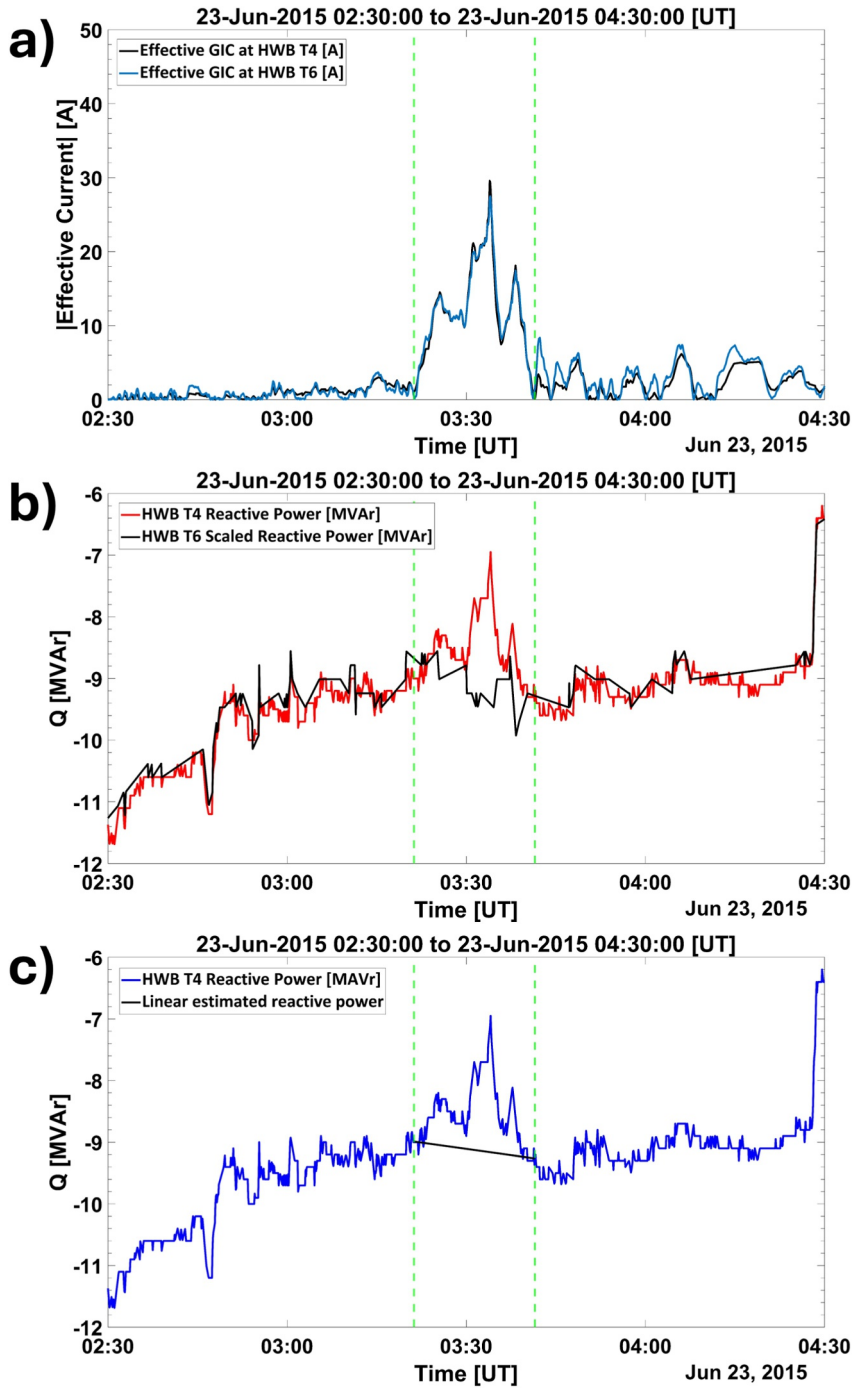

Figure 3. The variation of reactive power, *Q*, from 02:30–04:30 UT during 23 June 2015. Panel (a) shows the variation of GIC measured at the neutral—ground connection of transformer T4 (black line) and T6 (blue line). Vertical green dashed lines represent the start and end times of an enhanced GIC event. Panel (b) shows the variation of T4 *Q* values (red line) and the scaled T6 *Q* (black line). Deviations between the two data sets occur during the GIC event with the black line assumed to represent the background *Q* level during the GIC event. Panel (c) shows the variation of T4 *Q* values (blue line). A straight line fit between the start and end time of the enhanced GIC event (shown by vertical green dashed lines) is identified by the solid black line, and is a linear estimate of the background *Q* during the event.

Figure 6b shows the variation of T4 reactive power (red line) during the 2-hr window. Also shown is the scaled T6 reactive power variation (black line). Good agreement between the variation in T4 reactive power and the scaled T6 values can be seen for the first 30 min of the plot window, and the last 30 min. However, during the study

15427390, 2026, 6, Downloaded from https://agupubs.onlinelibrary.wiley.com/doi/10.1029/2026SW004966 by British Antarctic Survey, Wiley Online Library on [17/06/2026]. See the Terms and Conditions (https://onlinelibrary.wiley.com/terms-and-conditions) on Wiley Online Library for rules of use; OA articles are governed by the applicable Creative Commons License

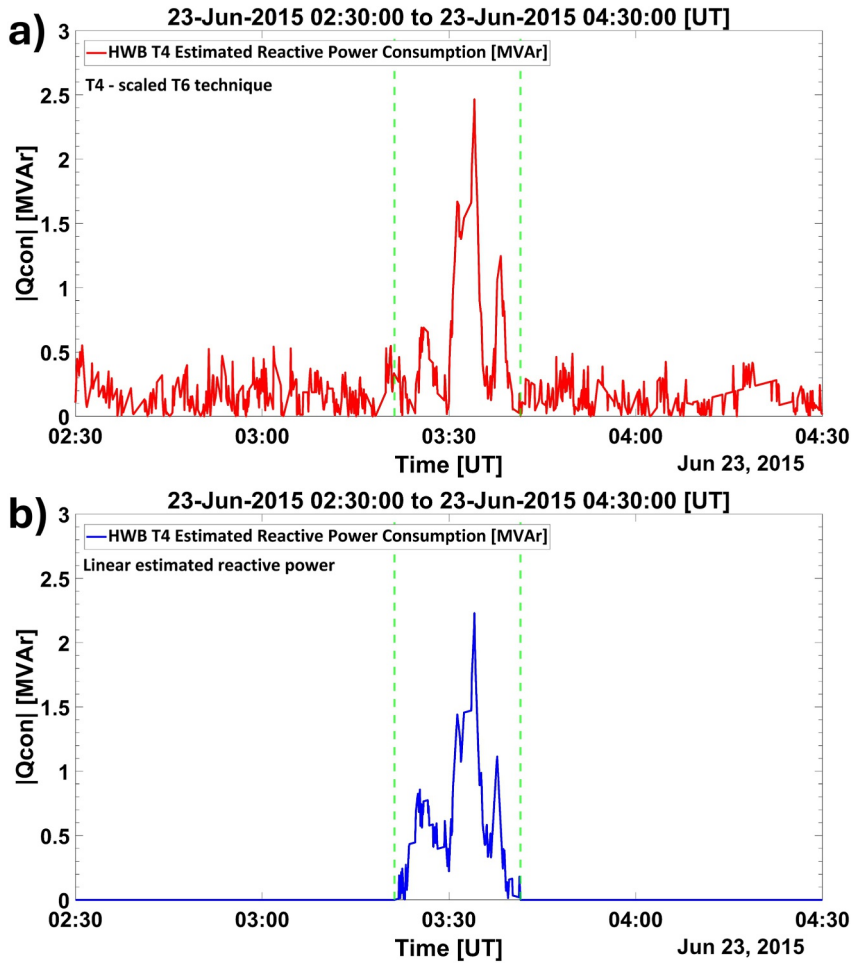

Figure 4. The variation of consumed reactive power, Q_{con}, in the single-phase transformer T4 during the 23 June 2015 GIC event, identified by the vertical green dashed lines. Panel (a) shows the variation of Q_{con} from T4 using the scaled T6 technique (red line), while panel (b) shows the variation of T4 Q_{con} using the linear estimated technique (blue line). Similar temporal features can be seen between the two panels, although higher Q_{con} levels occur using the scaled T6 technique.

period (indicated by the horizontal green lines) the T4 reactive power increases while the scaled T6 reactive power decreases initially and then stabilizes. The scaled T6 values during the study period are representative of the normal T4 reactive power variation under non-disturbed conditions, that is, they represent the T4 reactive power baseline. In Figure 6c T4 reactive power is again shown (blue line) during the 2-hr window, along with the study period. As in the previous case the baseline (black line) is calculated using a linear fit between the start and end times of the elevated GIC as shown in Figure 6a.

The differences between the two baseline techniques shown in Figures 6b and 6c are highlighted in Figure 7. Panel (a) shows the variation of the amplitude of the 4th harmonic of the fundamental AC frequency (50 Hz) during the September 2017 study period. For this event high time resolution even order harmonic observations were available (Clilverd et al., 2018), a very low frequency (VLF) receiver having been installed in 2016. The similarity to the GIC temporal variation shown in Figure 6a is consistent with half-cycle saturation of transformers in the HWB substation which would be expected to lead to increased reactive power consumption. Figure 7b shows the Q_{con} result from the scaled T6 technique, while Figure 7c shows the result from the linear estimate technique. Although there is some similarity in the temporal variation of Q_{con} using the two techniques, the scaled T6 technique shows larger Q_{con} values overall.

The 4th harmonic amplitude peak at ~12:45 UT in panel (a) is larger than the amplitude levels observed during the study period denoted by the green lines. This is consistent with the idea that at ~12:45 UT the effective GIC

15427390, 2026, 6, Downloaded from https://agupubs.onlinelibrary.wiley.com/doi/10.1029/2026SW004966 by British Antarctic Survey, Wiley Online Library on [17/06/2026]. See the Terms and Conditions (https://onlinelibrary.wiley.com/terms-and-conditions) on Wiley Online Library for rules of use; OA articles are governed by the applicable Creative Commons License

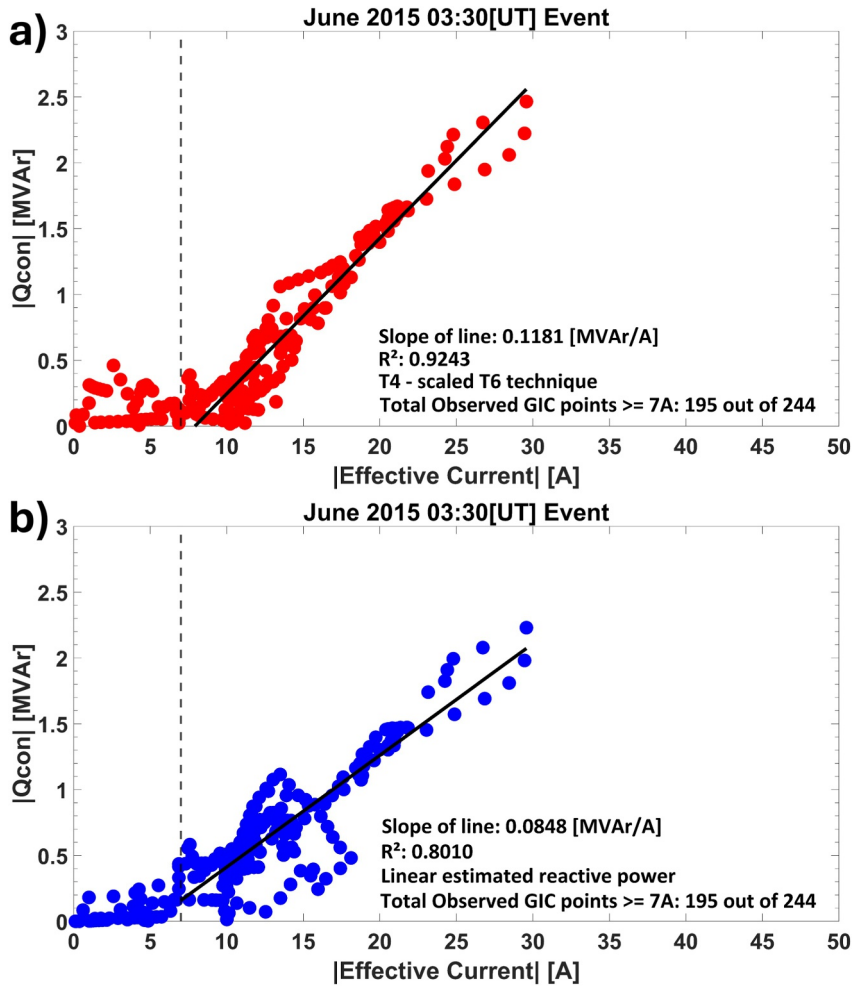

Figure 5. Plots of Q_{con} as a response to T4 effective GIC level during the 23 June 2015 GIC event. Panel (a) shows the results from the scaled T6 technique (red dots). A vertical dashed black line indicates an approximate "headroom" GIC level for T4. The slope and Pearson correlation coefficient, R^2, of the best fit line (solid black line) using datapoints where GIC ≥7 A are provided in the label. Panel (b) shows the results from the linear estimated technique (blue dots), with best fit slope and R^2 values provided in the label.

≥24 A in both T4 and T6, and thus both transformers would be contributing to the harmonic amplitude observed. The scaled T6 reactive power technique in panel (b) does not show such a large peak at 12:45 UT because T6 reactive power is enhanced above the background and thus it is being subtracted from the T4 reactive power at this time. The exclusion of the reactive power data from the analysis from just prior to 12:45 UT is due to the difficulty in identifying a clear scaled T6 background level when effective GIC ≥24 A in T6.

The relationship between effective GIC level and Q_{con} during the 08 September 2017 event is investigated in Figure 8. As in the previous analysis, values are only plotted from within the event period, as indicated by the green dashed lines shown in Figure 4. Panel (a) shows the relationship between effective GIC and the amplitude of the 4th harmonic of the fundamental mains frequency (50 Hz). Panel (b) shows the result from the scaled T6 technique, with a non-responsive region <7 A GIC, and a best fit slope of 0.110 MVAr/A with Pearson correlation ~0.85 for GIC ≥7 A. Panel (c) shows the result from the linear estimate technique. It exhibits a similar region of no response <7 A, and a best fit slope of 0.081 MVAr/A with Pearson correlation ~0.60 for GIC ≥7 A.

An additional period of enhanced GIC occurred on 08 September 2017, occurring at ~01:30 UT with peak effective currents of 16 A in T4, and 16 A in T6. Similar analysis using the scaled T6 and the linear estimate technique was undertaken (shown in Figure S1). The scaled T6 technique identified a best fit slope of 0.117 MVAr/A, while the linear estimate technique resulted in a best fit slope of 0.045 MVAr/A. These results are

15427390, 2026, 6, Downloaded from https://agupubs.onlinelibrary.wiley.com/doi/10.1029/2026SW004966 by British Antarctic Survey, Wiley Online Library on [17/06/2026]. See the Terms and Conditions (https://onlinelibrary.wiley.com/terms-and-conditions) on Wiley Online Library for rules of use; OA articles are governed by the applicable Creative Commons License

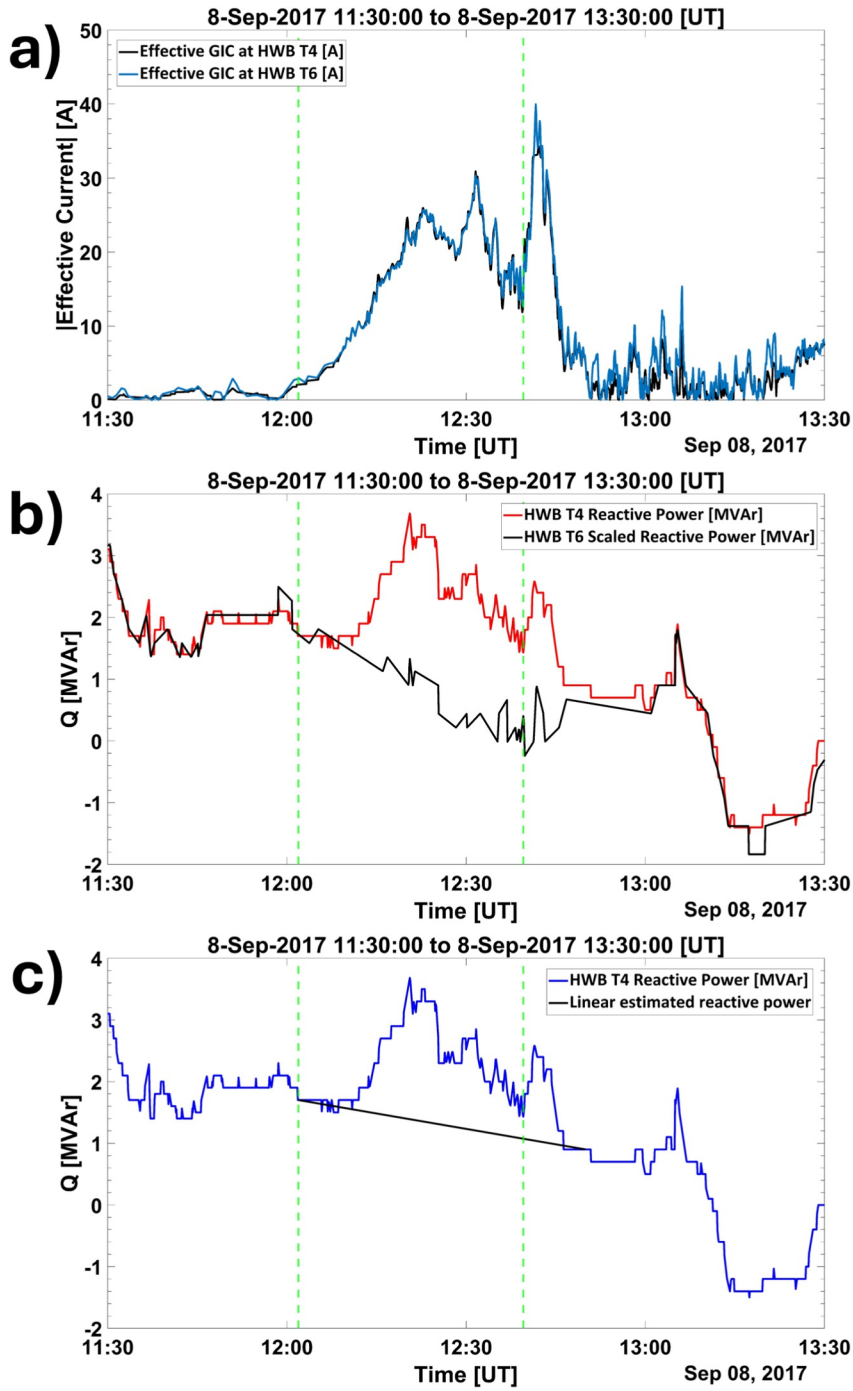

Figure 6. Same format as Figure 3 showing effective GIC and reactive power measurements for the period 11:30–13:30 UT on 08 September 2017. Vertical dashed green lines indicate the analysis period, which excludes a period of large currents in T6.

included in the analysis summary discussed in Section 5, and plots of the event are provided in a Supporting Information S1 file.

4.3. 2013–2015 Events Without T6 Present

Prior to June 2015 the three-phase, three-limb autotransformer T6 was not installed at HWB. Thus, the reactive power response of the single-phase T4 transformer can only be determined by applying the linear estimate

15427390, 2026, 6, Downloaded from https://agupubs.onlinelibrary.wiley.com/doi/10.1029/2026SW004966 by British Antarctic Survey, Wiley Online Library on [17/06/2026]. See the Terms and Conditions (https://onlinelibrary.wiley.com/terms-and-conditions) on Wiley Online Library for rules of use; OA articles are governed by the applicable Creative Commons License

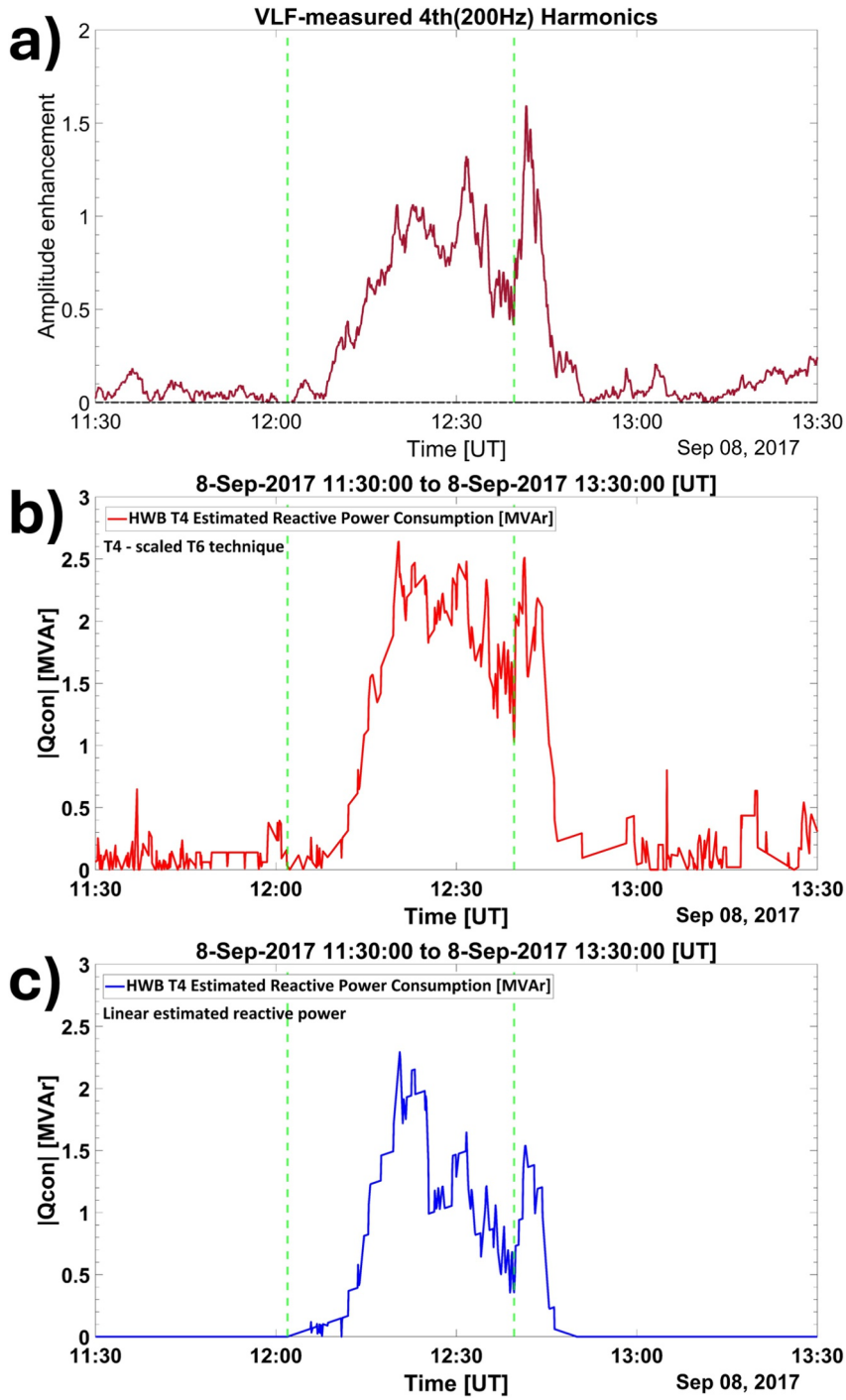

Figure 7. The variation of VLF-measured 4th harmonic amplitude from HWB substation, and consumed reactive power, Q_{con}, in the single-phase transformer T4 during the 11:30–13:30 UT 08 September 2017 GIC event, identified by the vertical green dashed lines. Panel (a) shows the variation of the 4th (i.e., even order) harmonic amplitude measured at the substation, confirming that half-cycle saturation is taking place. Panel (b) shows the variation of Q_{con} from T4 using the scaled T6 technique (red line), while panel (c) shows the variation of T4 Q_{con} using the linear estimated technique (blue line).

technique. Figure 9 summarizes 5 events spanning October 2013 to March 2015. The left-hand panels show the variations of T4 reactive power (blue lines) and T4 effective GIC levels over two-hour periods on 02 October 2013 and 17 March 2015. Peak effective GIC levels in T4 vary from ∼15 to ∼35 A, and five short-lived, spike-like events are identified by red labels. The application of the linear estimate technique to short-lived events should

15427390, 2026, 6, Downloaded from https://agupubs.onlinelibrary.wiley.com/doi/10.1029/2026SW004966 by British Antarctic Survey, Wiley Online Library on [17/06/2026]. See the Terms and Conditions (https://onlinelibrary.wiley.com/terms-and-conditions) on Wiley Online Library for rules of use; OA articles are governed by the applicable Creative Commons License

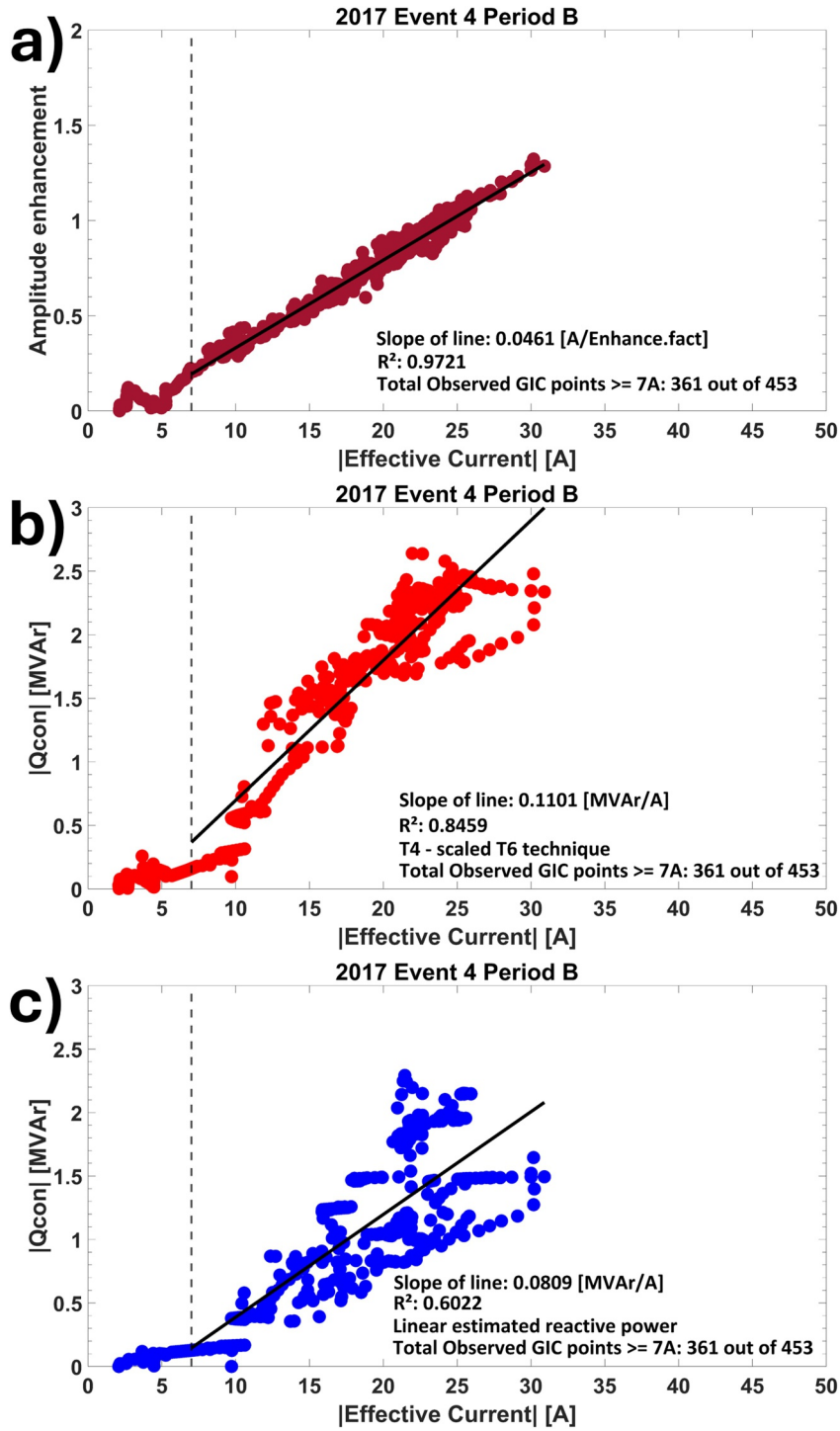

Figure 8. Plots of 4th harmonic amplitude, and Q_{con} as a response to T4 GIC level during the 08 September 2017 GIC event. Panel (a) shows the variation of the 4th (even order) harmonic amplitude. Panel (b) shows the results from the scaled T6 technique (red dots). The vertical dashed black line indicates the approximate "headroom" effective GIC level for T4. The slope and Pearson correlation coefficient, R^2, of the best fit line (solid black line) using datapoints where effective GIC ≥7 A are provided in the label. Panel (c) shows the results from the linear estimated technique (blue dots), with best fit slope and R^2 values provided in the label.

15427390, 2026, 6, Downloaded from https://agupubs.onlinelibrary.wiley.com/doi/10.1029/2026SW004966 by British Antarctic Survey, Wiley Online Library on [17/06/2026]. See the Terms and Conditions (https://onlinelibrary.wiley.com/terms-and-conditions) on Wiley Online Library for rules of use; OA articles are governed by the applicable Creative Commons License

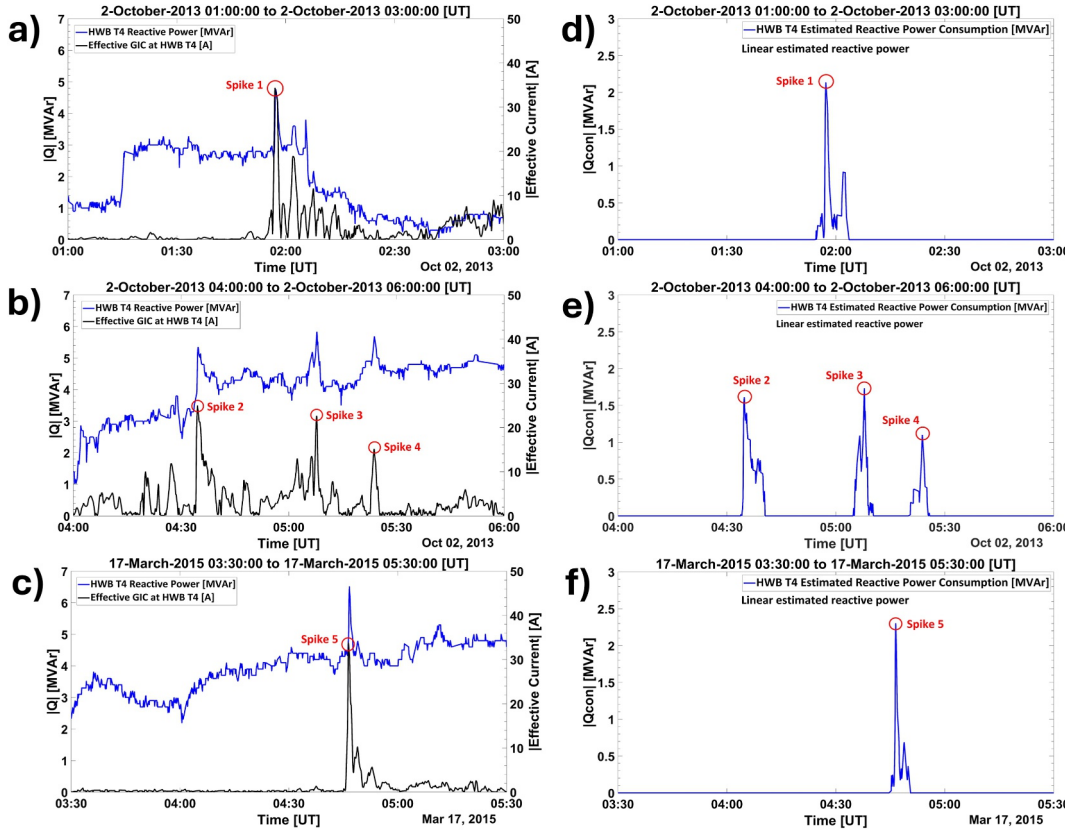

Figure 9. Showing the variation of Q (left-hand side) and Q_{con} (right-hand side) for five enhanced GIC events 2013–2015 where only the linear estimate technique could be applied. Effective GIC levels measured in T4 is shown by the black line in each panel (a)–(c). Q and Q_{con} are shown by the blue line. Five short-lived spike-like events are identified by red circular symbols with an accompanying label.

reduce the uncertainty in the estimation of the non-disturbed reactive power levels in the events. The right-hand panels show the reactive power consumption determined by subtracting a linear baseline estimate as described earlier in this study. Q_{con} peak levels of 1–2.5 MVAr occur close to the times of peak effective GIC in T4.

The reactive power consumption variation with GIC level in T4 for the five spike-like events is shown in Figure 10. As in previous analysis, a vertical dashed line indicates a potential 7 A "headroom" threshold effective GIC level, and a line of best fit is plotted for effective GIC values above that level. The slope of the line varies from 0.054 MVAr/A to 0.090 MVAr/A, with a typical value of 0.066 MVAr/A.

5. Discussion

The reactive power consumption of a single-phase autotransformer under the influence of enhanced GIC levels has been analyzed for 8 events where peak effective GIC > 15 A. Analysis of the T4 autotransformer at HWB has been undertaken using two different techniques to estimate the non-disturbed background levels of reactive power and thus estimate the reactive power consumption as a result of each GIC event. One technique assumes that it is possible to estimate the background using reactive power measurements from a nearby autotransformer, T6. An alternative technique assumes linear background variations in reactive power between periods when effective GIC levels are close to 0 A before and after the enhanced GIC event.

The results of the analysis are presented in Table 1. The enhanced GIC events are identified in the left-hand column and are presented in chronological order. Additional columns from left to right present the duration of the enhanced GIC event, the best fit reactive power consumption slope for the linear estimate technique when effective GIC ≥7 A, with an R^2 correlation coefficient of the fit, the best fit and R^2 correlation for the scaled T6 technique, and the maximum effective GIC level in T4 and T6 (when present) for each event. The last column in

15427390, 2026, 6, Downloaded from https://agupubs.onlinelibrary.wiley.com/doi/10.1029/2026SW004966 by British Antarctic Survey, Wiley Online Library on [17/06/2026]. See the Terms and Conditions (https://onlinelibrary.wiley.com/terms-and-conditions) on Wiley Online Library for rules of use; OA articles are governed by the applicable Creative Commons License

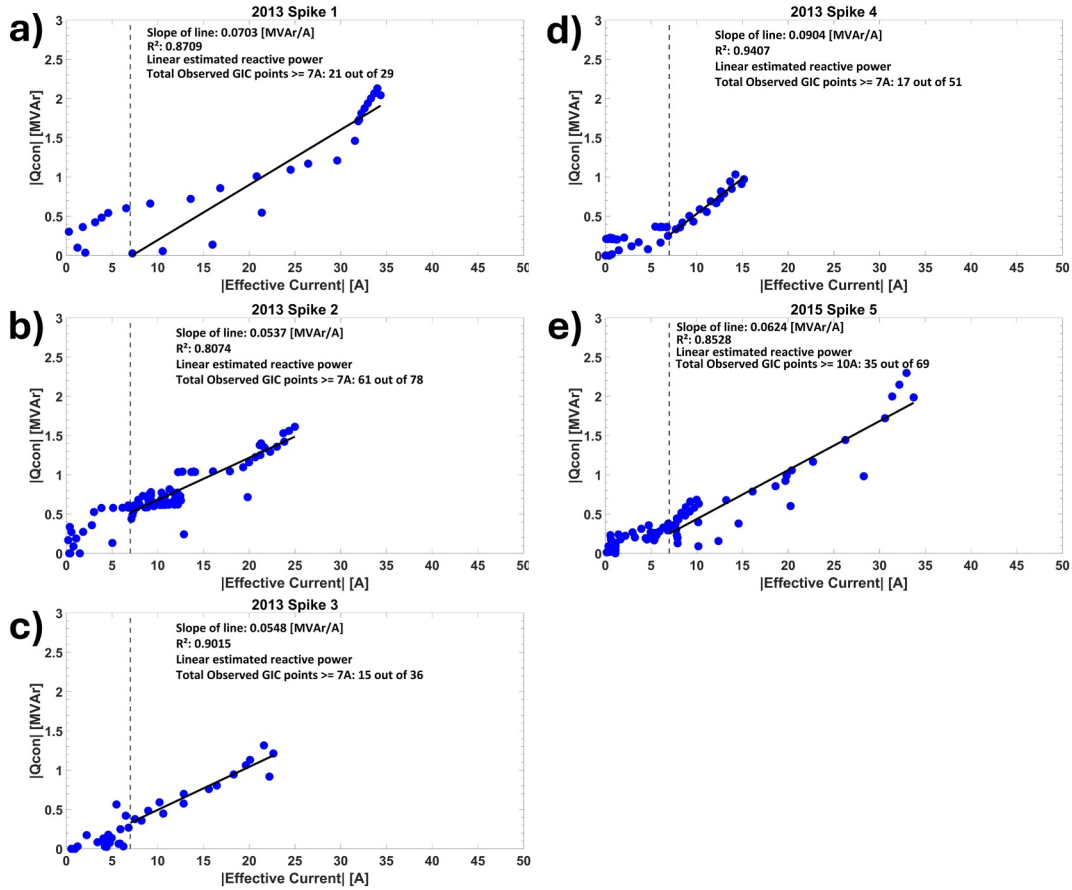

Figure 10. The variation of Q_{con} as a response to T4 effective GIC level during the five spike events identified in Figure 9. A vertical dashed black line indicates the approximate "headroom" GIC level for T4. The slope and Pearson correlation coefficient, R^2, of the best fit line (solid black line) using datapoints where effective GIC ≥7 A are provided in the label.

Table 1 shows the maximum *dH/dt* in nT/min for each event. The values are determined from magnetometer data recorded at Eyrewell (EYR) near Christchurch.

The table values show a weak relationship of increasing GIC level with increasing *dH/dt*, as has been found previously by Rodger et al. (2017) and Mac Manus et al. (2017). While an overall positive trend is expected, the correlation is not necessarily strong, especially when comparing event-level summary metrics (e.g., maximum *dH/dt* and maximum GIC) rather than time-resolved local quantities. In principle, larger geomagnetic field variations (which tend to result in higher *dH/dt*) produce stronger induced geoelectric fields, which can increase GIC. A detailed analysis of the correlation of *dH/dt* and GIC levels in transformers in New Zealand has been undertaken by Mac Manus et al. (2017) finding that although *dH/dt* is the dominant magnetic field factor for GIC, the overall disturbance in *H* is also well correlated to GIC level. However, the observed GIC at a specific transformer also depends on the power network line orientation. A high magnitude *dH/dt* event may result in modest GIC if the induction vector is misaligned with the primary orientation of the transmission lines.

All 8 events gave a reactive power consumption best fit slope using the linear estimate technique, while only 3 events were able to provide a slope via the scaled T6 technique. For the 3 events where the two techniques overlap, the slopes are substantially larger using the scaled T6 technique (an average of 0.115 MVAr/A c. f. 0.070 MVAr/A), and the average correlation coefficient is also higher. As expected, the short-lived spike events 1–5 show higher correlation coefficients than for the 3 longer-lasting events when using the linear estimate technique. We suggest this is due to a linear estimate to describe non-GIC reactive power changes being more applicable during short-lived spikes. For all 8 events the average linear estimated best fit slope is 0.068 MVAr/A, which is comparable to the average using the same technique for the 3 overlapping events. There are differences in the response slopes among the 8 events, that is, 0.045–0.090 MVAr/A, under the linear estimation reference

15427390, 2026, 6, Downloaded from https://agupubs.onlinelibrary.wiley.com/doi/10.1029/2026SW004966 by British Antarctic Survey, Wiley Online Library on [17/06/2026]. See the Terms and Conditions (https://onlinelibrary.wiley.com/terms-and-conditions) on Wiley Online Library for rules of use; OA articles are governed by the applicable Creative Commons License

15427390, 2026, 6, Downloaded from https://agupubs.onlinelibrary.wiley.com/doi/10.1029/2026SW004966 by British Antarctic Survey, Wiley Online Library on [17/06/2026]. See the Terms and Conditions (https://onlinelibrary.wiley.com/terms-and-conditions) on Wiley Online Library for rules of use; OA articles are governed by the applicable Creative Commons License

Table 1
A Summary of Results From All 8 Enhanced GIC Events Analyzed Using Measurements From the Single-Phase Autotransformer, T4, in HWB

Spike event	Duration	Slope (MVAr/A) (Linear estimated reactive power)	R^2 (Linear estimated reactive power)	Slope (MVAr/A) (T4—scaled T6 Technique)	R^2 (T4—scaled T6 Technique)	Maximum effective GIC in T4 (A)	Maximum effective GIC in T6 (A)	Maximum EYR dH/dt (nT/min)
2013 Spike 1	2 m 20 s	0.070	0.87	–	–	34	–	85.6
2013 Spike 2	6 m 25 s	0.054	0.81	–	–	25	–	53.0
2013 Spike 3	2 m 55 s	0.055	0.90	–	–	23	–	23.0
2013 Spike 4	4 m 10 s	0.090	0.94	–	–	16	–	16.5
2015 Spike 5	5 m 55 s	0.062	0.85	–	–	33	–	68.4
June 2015 03:30[UT] Event	16 m 55 s	0.085	0.80	0.118	0.92	30	28	11.9
2017 Event 3, Period A	29 m 25 s	0.045	0.47	0.117	0.80	16	16	14.5
2017 Event 4, Period B	37 m 40 s	0.081	0.60	0.110	0.85	31	30	20.0

Note. The event identifier, duration, reactive power response slope, and correlation coefficient for the linear estimate and scaled T6 techniques are provided. Additionally, the maximum effective GIC level in T4 and T6 (where appropriate) are given. For each event the maximum *dH/dt* (nT/min) is shown. The values are determined from magnetometer data recorded at New Zealand's official magnetometer observatory located at Eyrewell (EYR) near Christchurch.

method. The linear estimation method assumes that the normal background reactive power variation between the start and the end of each GIC-event linearly links the two points. Variations in system voltage, loading, and network conditions during events can change the normal reactive power level such that the background varies in a more complex way than a simple linear extrapolation provides. The addition of GIC-induced reactive power responses to the actual background behavior results in the linear estimation reference method giving response slope values that are not necessarily consistent from event to event (because of the assumption of simple linear background), and hence the range of slope values determined.

The T6 scaling technique uses reactive power measurements which are in close agreement with T4 reactive power measurements when no GIC are present and are thus expected to be more realistic than the linear estimate technique during GIC events. Consequently, a reactive power consumption response of ∼0.115 MVAr/A for effective GIC ≥7 A is the highest confidence result for the single-phase transformer, T4.

The GIC headroom for the three-phase, three-limb autotransformer, T6, in HWB was shown by Clilverd et al. (2025) to be ∼30 A based on measurements from the common winding. In Appendix A the effective GIC headroom for T6 was calculated to be 24 A. In the same Clilverd et al. study a similar headroom level was found for another three-phase, three-limb normal transformer, T3. Recently, Subritzky et al. (2026) determined a headroom level of ∼20 A for a three-phase, three-limb autotransformer during an active injection campaign in Wellington, New Zealand. In the current study of the single-phase autotransformer, T4, a headroom level of ∼7 A is indicated in Figures 4, 7 and 9 by a vertical dashed line. Although clearly identifiable in the panels in Figures 4 and 7, the 7 A headroom level is less obvious in some panels of Figure 10. Extrapolation of the lines of best fit in those figures to a $Q_{con} = 0$ effective GIC value suggests a headroom level between 5 and 10 A. The low headroom values obtained here for the single-phase transformer are consistent with the expected higher headroom thresholds of near-neighbor three-phase, three-limb transformers.

The reactive power response to GIC for the HWB single-phase autotransformer, T4, is 0.115 MVAr/A when using the scaled T6 technique. We suggest this is the most realistic estimate of the response slope compared with the simple linear estimate technique. In comparison to the three-phase, three-limb transformer units operated by Transpower Ltd in HWB, which gave results of 0.03–0.05 MVAr/A (Clilverd et al., 2025), the T4 response slope is more than a factor of two larger. The findings in this study, suggesting that single-phase transformers react to enhanced GIC starting at lower initial levels, and respond more to elevated GIC, is consistent with the modeling results of Dong et al. (2001) and power industry literature (Arrillaga and Watson (2003)). However, the gradient for the single-phase unit we determine from measurements is smaller than some modeling results predict, and the

15427390, 2026, 6, Downloaded from https://agupubs.onlinelibrary.wiley.com/doi/10.1029/2026SW004966 by British Antarctic Survey, Wiley Online Library on [17/06/2026]. See the Terms and Conditions (https://onlinelibrary.wiley.com/terms-and-conditions) on Wiley Online Library for rules of use; OA articles are governed by the applicable Creative Commons License

difference between single and three-phase, three-limb transformers is also less than modeling has predicted (i.e., a factor of 2 instead of 4; Dong et al., 2001). Marti et al. (2013) showed (in Figure 5) the Q_{con} -GIC response for 3 different operational voltages (450, 500, 550 kV) was about 0.4 MVAr/A. A simple linear fit to the three different response slopes shown suggests that a value of 0.115 MVAr/A for a single-phase transformer operating at 220 kV is consistent with a linear extrapolation from ∼500 to 220 kV. A factor of two increase in operational voltage compared to 220 kV results in a factor of ∼3 increase in responsiveness to GIC. Operational voltage is an important factor in the response of a power grid to enhanced GIC levels. However, the present study is primarily a transformer-specific case study in New Zealand (HWB T4), and the reported MVAr/GIC slopes are not intended as universal constants for all single-phase transformers.

The response of GIC-driven half-cycle saturation causing increased reactive power absorption in T4 depends on the specific transformer voltage level, design/structure, grounding/connection, and operating conditions. As such, a comparison of the measured reactive power/GIC relationship with modeling predictions, perhaps based on the Boteler et al. (1989) modeling framework, would be insightful. Unfortunately, detailed knowledge of the transformer design parameters, core geometry, magnetism curve and winding impedances are no longer available now that the unit has been taken out of service. However, a detailed modeling comparison for a known transformer with reactive power/GIC measurements available is a potential direction for future work.

We have shown that the GIC headroom and the fitted MVAr/GIC slope provide two measures relevant to the transformer saturation response for the T4 transformer at HWB. The headroom indicates the approximate onset level for T4 at which GIC begins to produce a measurable increase in reactive power demand, while the slope indicates the rate of reactive power increase per unit GIC once the response threshold is exceeded. However, the values found here should be interpreted as transformer and condition specific rather than universal constants. Their relevance should therefore be considered as contributing to the specification of transformer characteristics in broader system-level modeling studies, such as those assessing the response of a network to extreme space weather events (Mac Manus (2023); Mac Manus (2025)). In the context of the New Zealand high voltage power grid these findings do not significantly influence the estimate of total reactive power consumption during an extreme geomagnetic storm (Clilverd et al., 2025) as the majority of Transpower units are three-phase, three-limb and only a few units are single-phase. However, single-phase transformer units do add more to the reactive power burden on a network during geomagnetic storms compared to other transformer types. It is also important to note that the use of relatively low 220 kV operational voltages in New Zealand also reduces the system sensitivity to extreme GIC compared with many other countries. However, the identification of the T4 characteristic responses to GIC do confirm the findings of Crack et al. (2024) where single-phase units generated the majority of even order harmonics present in the power network during geomagnetic storms because of half-cycle saturation. As such, single-phase units can be a significant part of a power grid "route to blackout" via harmonics (Boteler, 2015; Boteler et al., 1989; Samuelsson, 2013).

6. Conclusions

Analysis has been made of reactive power measurements associated with the single-phase autotransformer, T4, in the Halfway Bush substation (HWB) in Dunedin, New Zealand. Adjustments in measured GIC were made to take into account the autotransformer winding configurations and expressed as effective GIC. During the period 2013–2017 a total of 8 short periods of enhanced GIC were observed, leading to reactive power responses. The events provide insight into the response of a single-phase autotransformer to elevated GIC during geomagnetic storms. The normal reactive power is highly variable because of the changes throughout the day in the power being transmitted to customers. This variability needs to be subtracted in determining the GIC-related reactive power response.. Here, the relationship between effective GIC level and reactive power consumption, Q_{con}, has been determined for the events using two different baseline techniques. To determine reactive power consumption a realistic baseline estimate is made when a nearby transformer shows similar normal reactive power variations during quiet times, but no response during moderately elevated GIC. The results from this baseline technique are compared to the results using a simple linear baseline estimate.

The following conclusions can be made:

1. To take into account autotransformer configuration an effective GIC is calculated to incorporate the effects of different values of GIC in the series and common windings. Effective GIC values of up to 30% different from

15427390, 2026, 6, Downloaded from https://agupubs.onlinelibrary.wiley.com/doi/10.1029/2026SW004966 by British Antarctic Survey, Wiley Online Library on [17/06/2026]. See the Terms and Conditions (https://onlinelibrary.wiley.com/terms-and-conditions) on Wiley Online Library for rules of use; OA articles are governed by the applicable Creative Commons License

the neutral–ground measured GIC levels are found for autotransformers in Halfway Bush substation, Dunedin, New Zealand.
2. The single-phase autotransformer, T4, starts to respond to enhanced effective GIC levels at ~7 A.
3. Realistic baseline estimates result in Q_{con}—GIC responses with higher correlations than a simple linear estimate for the background.
4. For effective GIC ≥7 A, the Q_{con} response of T4 is linear with a gradient of 0.115 MVAr/A.
5. At HWB, operating at 220 kV, the single-phase autotransformer reactive power consumption is triggered at lower GIC levels, and responds with larger gradients, than for similar voltage three-phase, three-limb transformer units located nearby.
6. The responsiveness of the single-phase unit operating at 220 kV is consistent with calculations made for similar transformers operating at higher voltages where gradients are expected to be larger.

In this study we have shown, as expected, the importance of a realistic removal of the normal background reactive power variation in order to determine the Q_{con} driven by GIC. Normal reactive power is shown to vary over a large range over short time periods due to the changes in the power transmitted to customers. A robust background removal technique is therefore necessary, and we find that the use of complementary measurements made within the same substation can provide the information required to reduce the effect of short-term variability. Once the background reactive power variation has been successfully removed the influence of GIC on single-phase transformer performance is readily identified and can be put into the framework of previous work.

Appendix A: T6 Effective Current Headroom During the May 2024 Gannon Storm

Clilverd et al. (2025) determined the T6 three-phase, three-limb transformer response to enhanced GIC at Halfway Bush substation in Dunedin, New Zealand, during the May 2024 Gannon geomagnetic storm. The transformer was found to show half-cycle saturation responses only when the measured GIC levels were ≥30 A. However, T6 is an autotransformer and, as shown in Section 2, it is important to use effective current as a measure of autotransformer sensitivity to GIC. This was not considered in Clilverd et al. (2025), who reported only the measured GIC, which represents the GIC in the common winding but not the series winding. In Section 2 the T6 effective current relationship to the measured GIC was determined for events occurring from 2015—2017. However, during the May 2024 Gannon Storm the network topology was different compared to the 2013–2017 period due to the removal of T4 and the introduction of T3 (Clilverd et al., 2018, 2025). This is likely to have changed the ratio of currents in the series and common windings of T6.

Here we use the GIC modeling results calculated as part of the analysis undertaken by Mac Manus et al. (2025) to calculate the T6 winding ratio μ_K during the Gannon storm in 2024. The ratio was found to be 0.57 ± 0.15, resulting in the relationship:

$$I_{\text{eff}} = 0.785\, I_{\text{common}}$$

This value is significantly lower than the 2015–2017 period where the correction factor was found to be 0.92 (see Section 2). Consequently, the headroom estimate of 30 A for T6 determined in from 2024 observation should be recalculated as an I_{eff} headroom threshold of 24 A. In Section 2, the T6 winding ratio was modeled as 0.86 ± 0.01. This was calculated for a network topology relevant to 2013–2017 and used a spatially uniform magnetic field due to measurement constraints. However, the 0.57 ± 0.15 winding ratio modeling for the May 2024 Gannon storm used a spatially varying magnetic field facilitated by multiple magnetic field measurements provided by the MANA network (Malone-Leigh et al., 2026). We tested the impact of using either a uniform or spatially varying magnetic field during the May 2024 Gannon storm. In both cases the T6 winding ratio showed a median value of 0.57, but the spatially varying magnetic field resulted in much larger variability in individual values (±0.15 compared with ±0.01 for the spatially uniform case).

Figure A1 recreates the T6 panel shown in Figure 9 of Clilverd et al. (2025) showing the effect of the transformer headroom to GIC but plotted as a function of effective current. The best fit line starts at 24 A, and the reactive power response slope is 0.049 MVAr/A—an increase on the Clilverd et al. (2025) slope result of 0.038 MVAr/A.

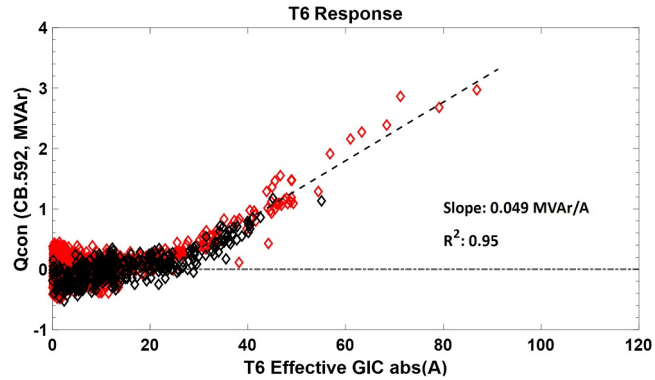

Figure A1. The variation of reactive power consumption (Q_{con}) in the three-phase, three-limb autotransformer T6 as a function of the effective GIC level during two enhanced GIC events (depicted by black and red symbols) in the May 2024 Gannon geomagnetic storm. The figure is equivalent to Figure 8, panel (b) in Clilverd et al. (2025) with effective GIC replacing measured GIC.

Conflict of Interest

The authors declare no conflicts of interest relevant to this study.

Availability Statement

The New Zealand LEM DC and reactive power data were provided to us by Transpower New Zealand with caveats and restrictions. This includes requirements of permission before all publications and presentations. In addition, we are unable to directly provide the New Zealand LEM DC data, derived GIC observations, or the reactive power data. Requests for access to the measurements need to be made to Transpower New Zealand. At this time the contact point is Michael Dalzell (Michael.Dalzell@transpower.co.nz). We are very grateful for the substantial data access they have provided, noting this can be a challenge in the Space Weather field (Hapgood & Knipp, 2016). The Halfway Bush VLF harmonic data for the 08 September 2017 events can be found at (Solar Tsunamis Team, 2025). Magnetometer data recorded at New Zealand's official magnetic observatory located at Eyrewell (EYR) near Christchurch is part of INTERMAGNET (http://www.intermagnet.org/) and is operated by GNS Science, New Zealand.

Acknowledgments
This research was supported by the New Zealand Ministry of Business, Innovation & Employment Endeavour Fund Research Programme Contract UOOX2002 and UOO2505. The authors would like to thank Transpower New Zealand for supporting this study. We would also like to thank Wayne Cleaver of Omexon New Zealand (previously Electrix Limited) for their assistance in facilitating the VLF measurements at Halfway Bush.

References

Albertson, V. D., Kappenman, J. G., Mohan, N., & Skarbakka, G. A. (1981). Load-flow studies in the presence of geomagnetically-induced currents. *IEEE Transactions on Power Apparatus and Systems*, *PAS-100*(2), 594–606. https://doi.org/10.1109/tpas.1981.316916

Arrillaga, J., & Watson, N. R. (2003). In *Power system harmonics* (2nd ed.). Wiley and Sons Ltd. https://doi.org/10.1002/0470871229

Beggan, C. D., Beamish, D., Richards, A., Kelly, G. S. P., & Thomson, A. W. (2013). Prediction of extreme geomagnetically induced currents in the UK high-voltage network. *Space Weather*, *11*(7), 407–419. https://doi.org/10.1002/swe.20065

Birkeland, K. (1908). *Norwegian Aurora polaris expedition, 1902-3 part 1*. H. Aschehoug and Company.

Bolduc, L., Gaudreau, A., & Dutil, A. (2000). Saturation time of transformers under dc excitation. *Electric Power Systems Research*, *56*(2), 95–102. https://doi.org/10.1016/S0378-7796(00)00087-0

Bonmann, D., Carrander, C., Kleivi, R., Ohnstad, T., Bjorgvik, G., & Susa, D. (2024). On-site GIC withstand experiment on a 1000 MVA autotransformer and a 300 MVA 5-limb transformer part II: Measurements and evaluation. International council on large electrical systems (CIGRE), Paris session, A2 power transformers and reactors (pp. 1–11).

Boteler, D. H. (2015). The impact of space weather on the electric power grid. In C. J. Schrijver, F. Bagenal, & Sojka (Eds.), *Heliophysics V. Space weather and society*. Lockheed Martin Solar and Astrophysics Laboratory.

Boteler, D. H., & Pirjola, R. J. (2017). Modeling geomagnetically induced currents. *Space Weather*, *15*(1), 258–276. https://doi.org/10.1002/2016SW001499

Boteler, D. H., Shier, R. M., Watanabe, T., & Horita, R. E. (1989). Effects of geomagnetically induced currents in the BC hydro 500 kV system. *IEEE Transactions on Power Delivery*, *4*(1), 818–823. https://doi.org/10.1109/61.19275

Clilverd, M. A., Rodger, C. J., Brundell, J. B., Dalzell, M., Martin, I., Mac Manus, D. H., et al. (2018). Long-lasting geomagnetically induced currents and harmonic distortion observed in New Zealand during the 7–8 September 2017 disturbed period. *Space Weather*, *16*(6), 704–717. https://doi.org/10.1029/2018SW001822

Clilverd, M. A., Rodger, C. J., Brundell, J. B., Dalzell, M., Martin, I., Mac Manus, D. H., & Thomson, N. R. (2020). Geomagnetically induced currents and harmonic distortion: High time resolution case studies. *Space Weather*, *18*(10), e2020SW002594. https://doi.org/10.1029/2020SW002594

15427390, 2026, 6, Downloaded from https://agupubs.onlinelibrary.wiley.com/doi/10.1029/2026SW004966 by British Antarctic Survey, Wiley Online Library on [17/06/2026]. See the Terms and Conditions (https://onlinelibrary.wiley.com/terms-and-conditions) on Wiley Online Library for rules of use; OA articles are governed by the applicable Creative Commons License

Clilverd, M. A., Rodger, C. J., Manus, D. H. M., Brundell, J. B., Dalzell, M., Renton, A., et al. (2025). Geomagnetically induced currents, transformer harmonics, and reactive power impacts of the Gannon storm in May 2024. *Space Weather*, *23*(4), e2024SW004235. https://doi.org/10.1029/2024SW004235

Crack, M., Rodger, C. J., Clilverd, M. A., Mac Manus, D. H., Martin, I., Dalzell, M., et al. (2024). Even-order harmonic distortion observations during multiple geomagnetic disturbances: Investigation from New Zealand. *Space Weather*, *22*(5), e2024SW003879. https://doi.org/10.1029/2024SW003879

Divett, T., Ingham, M., Beggan, C. D., Richardson, G. S., Rodger, C. J., Thomson, A. W. P., & Dalzell, M. (2017). Modeling geoelectric fields and geomagnetically induced currents around New Zealand to explore GIC in the south Island's electrical trans-mission network. *Space Weather*, *15*(10), 1396–1412. https://doi.org/10.1002/2017SW001697

Divett, T., Mac Manus, D. H., Richardson, G. S., Beggan, C. D., Rodger, C. J., Ingham, M., et al. (2020). Geomagnetically induced current model validation from New Zealand's south island. *Space Weather*, *18*(8), e2020SW002494. https://doi.org/10.1029/2020SW002494

Divett, T., Richardson, G. S., Beggan, C. D., Rodger, C. J., Boteler, D. H., Ingham, M., et al. (2018). Transformer-level modelingof geomagnetically induced currentsin New Zealand's South Island. *Space Weather*, *16*, 718–735. https://doi.org/10.1029/2018SW001814

Dong, X., Liu, Y., & Kappenman, J. G. (2001). Comparative analysis of exciting current harmonics and reactive power consumption from GIC saturated transformers. *2001 IEEE Power Engineering Society Winter Meeting. Conference Proceedings (Cat. No.01CH37194)*, *1*, 318–322. https://ieeexplore.ieee.org/document/917055

Hapgood, M., & Knipp, D. J. (2016). Data citation and availability: Striking a balance between the ideal and the practical. *Space Weather*, *14*(11), 919–920. https://doi.org/10.1002/2016SW001553

Mac Manus, D. H., Rodger, C. J., Dalzell, M., Renton, A., Richardson, G. S., Petersen, T., & Clilverd, M. A. (2022). Geomagnetically induced current modeling in New Zealand: Extreme storm analysis using multiple disturbance scenarios and industry provided hazard magnitudes. *Space Weather*, *20*(12), e2022SW003320. https://doi.org/10.1029/2022SW003320

Mac Manus, D. H., Rodger, C. J., Dalzell, M., Thomson, A. W. P., Clilverd, M. A., Petersen, T., et al. (2017). Long-term geomagnetically induced current observations in New Zealand: Earth return corrections and geomagnetic field driver. *Space Weather*, *15*(8), 1020–1038. https://doi.org/10.1002/2017sw001635

Mac Manus, D. H., Rodger, C. J., Renton, A., Lo, V., Malone-Leigh, J., Petersen, T., et al. (2025). Implementing geomagnetically induced currents mitigation during the May 2024 "Gannon" G5 storm: Research informed response by the New Zealand power network. *Space Weather*, *23*(6), e2025SW004388. https://doi.org/10.1029/2025SW004388

Mac Manus, D. H., Rodger, C. J., Renton, A., Ronald, J., Harper, D., Taylor, C., et al. (2023). Geomagnetically induced current mitigation in New Zealand: Operational mitigation method development with industry input. *Space Weather*, *21*(11), e2023SW003533. https://doi.org/10.1029/2023sw003533

Malone-Leigh, J., Rodger, C. J., Hendry, A. T., Brundell, J., Mac Manus, D., Petersen, T., et al. (2026). The MANA magnetometer array, and magnetic observations across New Zealand from 2024. *Space Weather*, *24*(2), e2025SW004629. https://doi.org/10.1029/2025SW004629

Marshall, R. A., Dalzell, M., Waters, C. L., Goldthorpe, P., & Smith, E. A. (2012). Geomagnetically induced currents in the New Zealand power network. *Space Weather*, *10*(8), S08003. https://doi.org/10.1029/2012SW000806

Marti, L., Berge, J., & Varma, R. K. (2013). Determination of geomagnetically induced current flow in a transformer from reactive power absorption. *IEEE Transactions on Power Delivery*, *28*(3), 1280–1288. https://doi.org/10.1109/TPWRD.2012.2219885

Patil, K. (2014). Modeling and evaluation of geomagnetic storms in the electric power system. In *Paper C4-306 presented at CIGRE 2014*.

Price, P. R. (2002). Geomagnetically induced current effects on transformers. *IEEE Transactions on Power Delivery*, *17*(4), 1002–1008. https://doi.org/10.1109/MPER.2002.4312311

Rezaei-Zare, A. (2014). Behavior of single-phase transformers under geomagnetically induced current conditions. IEEE transactions on power delivery. *IEEE Transactions on Power Delivery*, *29*(2), 916–925. https://doi.org/10.1109/TPWRD.2013.2281516

Rezaei-Zare, A., Marti, L., Narang, A., & Yan, A. (2016). Analysis of three-phase transformer response due to GIC using an advanced duality-based model. *IEEE Transactions on Power Delivery*, *31*(5), 2342–2350. https://doi.org/10.1109/TPWRD.2015.2505499

Rodger, C. J., Clilverd, M. A., Mac Manus, D. H., Martin, I., Dalzell, M., Brundell, J. B., et al. (2020). Geomagnetically induced currents and harmonic distortion: Storm-time observations from New Zealand. *Space Weather*, *18*(3), e2019SW002387. https://doi.org/10.1029/2019SW002387

Rodger, C. J., Mac Manus, D. H., Dalzell, M., Thomson, A. W. P., Clarke, E., Petersen, T., et al. (2017). Long-term geomagnetically induced current observations from New Zealand: Peak current estimates for extreme geomagnetic storms. *Space Weather*, *15*(11), 1447–1460. https://doi.org/10.1002/2017SW001691

Samuelsson, O. (2013). Geomagnetic disturbances and their impact on power systems. Industrial electrical engineering and automation, lund university.

Solar Tsunamis Team. (2025). VLF wideband data from Dunedin, 08 September 2017 [Dataset]. *Zenodo*. Retrieved from https://zenodo.org/record/1246869#.WvoINXWFOK5

Subritzky, S., Lapthorn, A., Hardie, S., Agger, P., Dalzell, M., Clilverd, M. A., et al. (2026). High voltage DC active current injection to simulate geomagnetically induced currents in New Zealand. *Space Weather*, *24*(3), e2025SW004681. https://doi.org/10.1029/2025SW004681

Vasseur, G., & Weidelt, P. (1977). Bimodal electromagnetic induction in non-uniform thin sheets with an application to the northern Pyrenean induction anomaly. *Geophysical Journal International*, *51*(3), 669–690. https://doi.org/10.1111/j.1365-246X.1977.tb04213.x

15427390, 2026, 6, Downloaded from https://agupubs.onlinelibrary.wiley.com/doi/10.1029/2026SW004966 by British Antarctic Survey, Wiley Online Library on [17/06/2026]. See the Terms and Conditions (https://onlinelibrary.wiley.com/terms-and-conditions) on Wiley Online Library for rules of use; OA articles are governed by the applicable Creative Commons License